JOURNAL OF CATALYSIS 132, 68–78 (1991)

Kinetic Study of Ethylene Dimerization Catalyzed over $Ti(O-nC_4H_9)_4/AlEt_3$

TAE W. WOO AND SEONG I. WOO[1]

Department of Chemical Engineering, Korea Advanced Institute of Science of Technology, P.O. Box 150, Cheongryang, Seoul, Korea

Received November 20, 1990; revised March 21, 1991

Dimerization of ethylene to 1-butene catalyzed by $Ti(O-nC_4H_9)_4-AlEt_3$ was investigated. The kinetics in the initial period and of deactivation were studied at various aluminum alkyl concentrations. The mechanisms of formation of active sites and deactivation were discussed. Deactivation is ascribed to the oligomerization of active sites with aluminum alkyl. The number of active sites was determined by the CO-poisoning method. The maximum number of active sites is 35% of total titanium at 303 K and the Al/Ti molar ratio of 5.4. The rate constant of dimerization (k_D), was found to be 75.2 liter/mol sec. The active site for dimerization of ethylene is believed to be uniform as expected from the soluble mixture of catalytically active species.

INTRODUCTION

Most of industrial olefin polymerization catalysts are based on titanium butoxide/aluminum alkyl or titanium tetrachloride/aluminum alkyl. The catalytic active species obtained from titanium butoxide and aluminum alkyls, precursors of active Ziegler–Natta catalysts, are too complicated and unstable to be isolated. One of the perplexing problems in these catalyst systems is a characterization of catalytically active species produced from the reaction of titanium compound with aluminum alkyls. The titanium alkoxide/trialkylaluminum catalytic system is known to be a homogeneous system for polymerization of ethylene (*1*), styrene (*2*), and conjugated dienes (*3–7*). This catalyst system dimerizes ethylene selectively to butenes, mainly 1-butene (*8–10*).

Pillai *et al.* (*8*) investigated dimerization of ethylene to 1-butene catalyzed by $Ti(O-nC_4H_9)/AlR_3$ ($R = CH_3, C_2H_5, iC_4H_9$) in a batch reactor. They studied the influence of reaction conditions such as Al/Ti molar ratio, pressure, temperature, and the addition of polar compounds on the initial rate of dimerization and the selectivity to 1-butene. Beach and Kissin (*9, 10*) also studied the kinetics of dimerization of ethylene for *in situ* 1-butene production during ethylene/1-butene copolymerization in a semibatch reactor. They observed both first- and second-order deactivations for the $Ti(OR)_4/AlEt_3$ catalytic system.

In the present paper, the effects of such reaction parameters as Al/Ti molar ratio, pressure, and temperature on the kinetics of dimerization of ethylene were examined in a semibatch reactor.

From the analysis of rate profiles, the mechanism of active site formation and plausible catalytically active species during dimerization was discussed. The number of active sites was measured by the CO-poisoning method to determine the dimerization reaction rate constant (k_D).

EXPERIMENTAL

Materials

Ethylene (polymer grade, Matheson, USA) and nitrogen of extrapure grade were further purified with the columns of Fisher Ridox and molecular sieves 5A and 13X.

---

[1] To whom all correspondence should be addressed.

0021-9517/91 $3.00

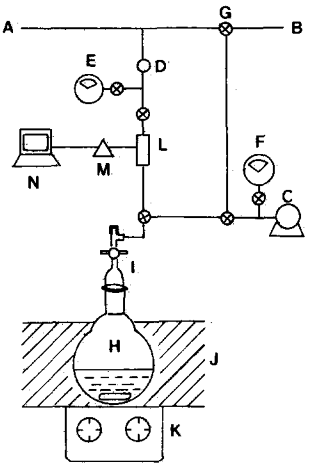

FIG. 1. Ethylene dimerization reactor system: (A) ethylene inlet; (B) nitrogen inlet; (C) vacuum pump; (D) pressure regulator; (E) pressure gauge; (F) vacuum gauge; (G) valves; (H) reactor; (I) inlet adapter; (J) constant temperature bath; (K) magnetic stirrer; (L) mass flowmeter; (M) A/D converter; (N) personal computer.

n-Hexane (extra-pure grade, Duksan Ltd., Korea) was refluxed over sodium metal with benzophenone and distilled under a slightly positive nitrogen pressure. Triethylaluminum (25 wt% solution in toluene, Aldrich) and titanium butoxide, monomeric (99%, Tokyo Chem., Japan) were used without further purification.

Procedure

Dimerization was carried out in a two-neck 500-ml or 250-ml flask equipped with an ethylene inlet tube and a magnetic stirrer. The schematic diagram of the dimerization reactor system is shown in Fig. 1. After several evacuations and nitrogen purges, 100 ml of *n*-hexane was introduced into the reactor under nitrogen stream. A prescribed amount of triethylaluminum was introduced. Nitrogen was purged with ethylene under slight positive ethylene pressure and ethylene was saturated into *n*-hexane at the dimerization temperature. Dimerization was started by injection of the prescribed amount of the titanium butoxide. The dimerization mixture was agitated with a magnetic bar at 1200 rpm; this prevented mass transfer resistance through vapor–liquid interface. The temperature of the dimerization was controlled within 0.5°C. The rate of ethylene consumption was measured with a mass flow meter (Sierra, Model 820) connected to a personal computer through a A/D converter every 0.02 sec. This is equivalent to rate of dimerization. A HP-5890 chromatograph equipped with a methyl silicone (cross-linked)-coated capillary column and a flame ionization detector was used for analysis of products in the reactor.

RESULTS AND DISCUSSION

Absence of Gas–Liquid Mass Transfer Resistance

If the gas–liquid mass transfer rate is smaller than the intrinsic reaction rate, it is impossible to perform a kinetic study. To determine the concentration of the catalyst at which gas–liquid mass transfer resistance is absent, dimerization was carried out with various concentrations of titanium butoxide with a constant Al/Ti molar ratio. Figure 2 shows that the gas–liquid mass transfer resistance is negligible below a concentration of titanium butoxide of 2.0 mmol/liter.

During dimerization reaction, an accumulation of dimerized products in the reactor can cause a decrease in the partial pres-

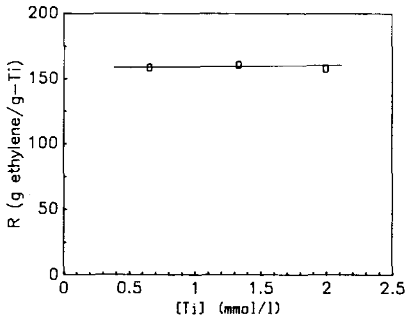

FIG. 2. Average activities over 1 hr with various $Ti(n\text{-}OBu)_4$ concentrations. Dimerization condition: $T = 303$ K, $P_t = 1.16$ atm, Al/Ti molar ratio = 18.8.

sure of ethylene because the total reaction pressure was kept constant. The rate profiles of two different sizes of reactor having different surface to volume ratios (100 ml *n*-hexane in a 250-ml one-neck flask and 500-ml two-neck flask) were nearly same. Hence it can be concluded that a small decrease in the ethylene partial pressure does not affect significantly the reaction rate in our experimental conditions. The amounts of solvent medium, i.e., 100 ml and 200 ml in a two-neck 500-ml flask, did not affect the rate profiles. From the ethylene consumption data or GC analysis of solution, X_B (mol fraction of 1-butene in liquid phase) can be determined. The vapor-phase analysis by GC measured the partial pressure of ethylene (P_E). C_E can be calculated with Eq. (1) based on Henry's law, obtained by data fitting (*11*).

$$C_E \text{ (mol/liter)} = (A + B\,X_B)\,P_E, \quad (1)$$

where X_B is the mol fraction of 1-butene in the liquid phase, $A = 0.1162$ (mol/liter/atm), and $B = 0.1280$ (mol/liter/atm) at 303 K.

The small decrease in P_E is compensated for by the increase in Henry's constant ($A + B\,X_B$) due to the $B\,X_B$ term, to give a nearly constant C_E throughout the reaction.

Reaction Product Distribution

The vapor phase in the reactor was sampled and analyzed with a gas chromatograph equipped with a methyl silicone (cross-linked)-coated capillary column and a flame ionization detector. The liquid phase, after quenching with a mixture of ethanol and HCl, was analyzed for the analysis of hexenes, octenes, and oligomers. The amounts of solid products were determined after filtration. The products of the reaction at various ratios of Al/Ti (5.4, 10.7, 13.4, 18.8, and 21.5) contain exclusively 1-butene (>97%), small amounts of hexenes, and negligible solid product (<2%). The products in the reaction of ethylene catalyzed over titanium(IV) butoxide and triethylaluminum were found to be dependent on the reaction parameters, especially on the Al/Ti molar ratio and temperature (*8*). However, this was not the case under our experimental conditions. The selectivity to 1-butene in our experiments is much higher than that in Pillai *et al.*'s experiments (*8*). They reported that selectivity to 1-butene is 75–78 wt% when Al/Ti molar ratio is 7.6 and reaction temperature is 299 K. Other products include hexenes, octenes, and polymers. This discrepancy could be easily explained by indications that the activity of olefin oligomerization catalyzed over zirconium tetrachloride ester complex or zirconium tetra-*n*-propoxide with diethylaluminum chlorides is strongly dependent on the presence of Zr–O–Zr or Al–O–Al linkages resulting from traces of water (*12*). The water contamination in the experiment of Pillai *et al.* might cause lower selectivity to 1-butene. Another reason might be the fact that Pillai *et al.* used a batch reactor and we used a semibatch reactor. The increase in concentration of 1-butene and decrease in C_E in the batch process can facilitate codimerization of ethylene with 1-butene to produce hexenes and dimerization of 1-butene to make octenes (*13*). Beach and Kissin (*10*) reported the product distribution of 1-butene (>90%), 2-butenes (*cis, trans,* 1.5%), hexenes, and a small amount of linear polyethylene (ca. 2–4%). Considering the fact that the selectivity to 1-butene decreases with an increase in reaction temperature (*8*), and that our reaction temperature (303–333 K) was lower than that of Beach and Kissin (363 K), our result is agreeable with the result of Beach and Kissin.

Effect of Al/Ti Molar Ratio on Average Rate

Figure 3 shows the average activity during 1 hr at various Al/Ti molar ratios. Below Al/Ti molar ratio of 2.1, dimerization did not occur. Pillai *et al.* (*8*) also reported that dimerization does not occur below a Al/Ti molar ratio of about 2.0. And the

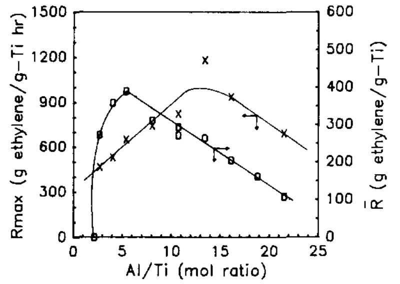

FIG. 3. Average activities for 1 hr (O) and maximum rate of dimerization (×) with variation of Al/Ti molar ratios. Dimerization condition: $T = 303$ K, $P_t = 1.16$ atom, Ti = 1.33 mmol/liter.

polymerization of styrene was reported to be negligible below Al/Ti molar ratio of two (*2*). This fact must be ascribed to the dependence of the formation of catalytically active titanium–aluminum complexes on the Al/Ti molar ratio.

The structures of the products obtained in the reaction of titanium alkoxide with aluminum alkyl were investigated by several authors (*14–16*). Djabiev *et al.* (*14*) found an ESR signal with a *g*-value of 1.957 and a hyperfine structure at a Al/Ti molar ratio of two, and thus concluded that this ESR band was ascribed to the formation of complex.

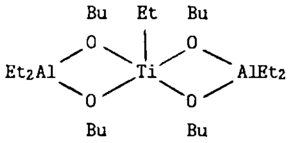

(I)

Hirai *et al.* (*15*) also examined titanium butoxide–triethyl aluminum complex with ESR spectroscopy to determine the structures of the products obtained at various of Al/Ti molar ratios. They proposed other kinds of complexes:

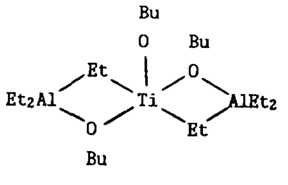

(II)

(Al/Ti < 2)

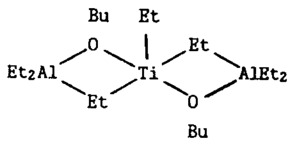

(III)

(Al/Ti > 3)

According to chemical ionization mass spectrometric (CI–MS) data (*16*), the reaction of $Al(CH_3)_3$ with $Ti(O\text{–}iC_3H_7)_4$ resulted in the formation of three main complexes:

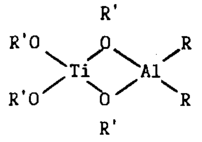

(Al/Ti < 1)

(IV)

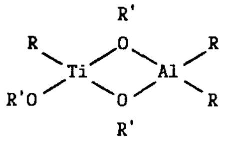

(Al/Ti > 2)

(V)

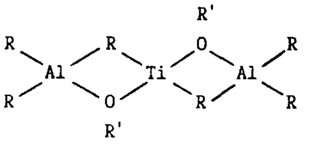

R = CH_3
R' = $CH(CH_3)_2$

(Al/Ti > 10)

(VI)

The formal oxidation states of Ti in complexes (V) and (VI) are +3 and +2, respectively. These complexes have a Ti–C bond that is the catalytically active dimerization center. It has long been accepted that the active species for the oligomerization and polymerization of α-olefin should have a Ti–C bond containing species (*17, 18*). Complex (IV) is not active because it was prepared at the Al/Ti molar ratio of less than 1. Figure 3 indicated that there is no dimerization reaction at the Al/Ti molar ratio of less than 2. Hence we can propose that the primary catalytically active complex in the reaction of titanium butoxide with triethyl aluminum is complex (V). Figure 3 also shows that the maximum average activity for 1 hr is obtained at the Al/Ti molar ratio of 5.3. The activity of the dimerization catalyst is strongly dependent on Al/Ti molar ratio. The relative concentrations of complexes (IV), (V), and (VI) in equilibrium at various Al/Ti molar ratios are responsible for the variation in catalytic activity.

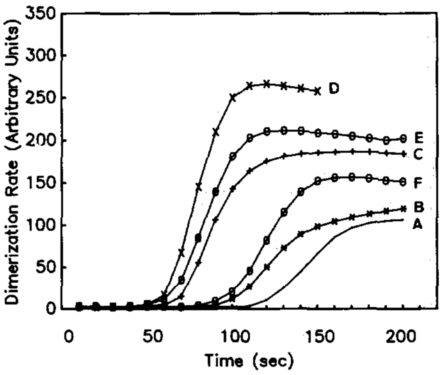

FIG. 4. Rate profiles of dimerization at the initial period at various Al/Ti molar ratios. The dimerization condition is the same as that in Fig. 3. Al/Ti molar ratio: (A) 2.7; (B) 4.02; (C) 10.7; (D) 13.4; (E) 16.1; (F) 21.5.

Effect of Al/Ti Molar Ratio on the Dimerization Rate in the Initial Period

Figure 4 shows the rate profiles of dimerization at the initial period. After the short induction period, the rate reaches its maximum value. When the Al/Ti molar ratio increases, the induction period becomes shorter and the maximum rate of dimerization becomes greater. However, when the Al/Ti molar ratio is greater than 13.4, the induction period becomes longer and the maximum rate of dimerization decreases. The induction time is a period for the formation of preactive sites. When the Al/Ti molar ratio is higher than 2.1, the mechanism for the formation of preactive sites can be proposed as follows:

$$\mathrm{Al_d} \rightleftharpoons 2\mathrm{Al_m} \tag{2}$$

$$\mathrm{Al_m} + \mathrm{Ti(O\text{-}}n\mathrm{C_4H_9)_4} \xrightarrow{-R} C_1, \tag{3}$$

where $\mathrm{Al_d}$ is the dimeric form of triethyl aluminum, $\mathrm{Al_m}$ is the monomeric form of triethyl aluminum, C_1 represents the preactive sites being active with further reaction with aluminum alkyl, and R represents C_2H_5.

The first two steps were suggested by Christenson *et al.* (*16*). Preactive sites, C_1 can be assumed to have a (IV)-like structure. Table 1 shows the kinetic parameters of dimerization at various Al/Ti molar ratios in the initial period. The maximum rates of dimerization at various Al/Ti molar

TABLE 1

Kinetic Parameters of Dimerization at Initial Period with Various Al/Ti Molar Ratios (Dimerization Condition: T = 303 K, C_M = 0.1067 mol/liter, Ti = 1.33 mmol/liter)

Al/Ti (mol ratio)	t_i[a] (sec)	t_{max}[b] (sec)	R_{max} (g C_2/g Ti, hr)	$t_{1/2}$[c] (sec)	$k_i \times 10^3$ (sec^{-1})
2.7	100	210	466	144	15.8
4.0	80	200	529	124	15.8
5.4	70	190	649	114	15.8
8.1	50	150	740	95	15.5
10.7	50	150	823	87	18.7
13.4	30	120	1180	78	14.5
16.1	40	120	934	84	15.8
21.5	70	170	690	119	14.2

[a] Induction period.

[b] Time to reach the maximum rate of dimerization.

[c] Time to reach half of the maximum rate of dimerization.

ratios are plotted in Fig. 3. The sigmoidal increase in the rate of the dimerization can be interpreted to mean that preactive sites are transformed to the active sites in the following mechanism (*19*).

$$C_1 \overset{K}{\rightleftharpoons} \mathrm{Ti}(\mathrm{O}R')_3 + \mathrm{Al}(\mathrm{O}R')R_2 \quad (4)$$

$$\mathrm{Ti}(\mathrm{O}R')_3 + \mathrm{Al_m} \xrightarrow{k_i} C^*, \quad (5)$$

where C^* represents the active sites.

This sigmoidal increase in the rate of dimerization can be expressed by

$$(R_{\max} - R)/R_{\max} = \mathrm{Exp}[-k_i\,(t - t_i)], \quad (6)$$

where, $R_{\max}$ is the maximum dimerization rate, R is the dimerization rate at time t, and t_i is the induction time.

From the value of $t_{1/2}$, the time at which R reaches the half of $R_{\max}$, k_i can be calculated from the relation of $k_i = 0.6963/(t_{1/2} - t)$. The dimerization rate profiles at various Al/Ti molar ratios were fitted well to Eq. (6). As shown in Table 1, the values of k_i are in the range between 14.2 and 15.8 irrespective of the Al/Ti molar ratio, indicating that this proposed mechanism is kinetically reasonable. The following conclusions can be made from these kinetic results:

1. The induction period is necessary for the formation of preactive sites. The preactive sites can be more rapidly formed at higher aluminum alkyl concentration.
2. The preactive sites are converted to active sites by further reaction with aluminum alkyl.
3. At a very high concentration of aluminum alkyl (Al/Ti > 13), formation of less active sites occurs which causes the induction time to increase and the maximum rate of dimerization to decrease. This could be due to the fact that many kinds of Al–Ti complexes can be formed at a very high Al/Ti molar ratio (*15*).

Effect of Monomer Concentration on the Maximum Rate of Dimerization

The maximum rate of dimerization is proportional to the monomer concentration, as shown in Fig. 5. This is in agreement with a kinetic scheme in which insertion of ethylene into active sites is rate determining for dimerization reaction.

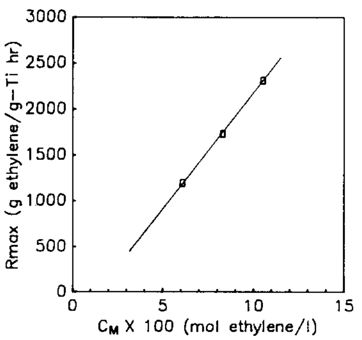

FIG. 5. Plot of maximum rates of dimerization with ethylene concentration. Dimerization condition: T = 323 K, Al/Ti = 21.5, Ti = 1.33 mmol/liter.

Effect of Temperature on the Maximum Rate of Dimerization

The effect of temperature on the maximum rate of dimerization was studied in the temperature range of 30–60°C. The Al/Ti molar ratio was 9.2. Table 2 shows the maximum rates of dimerization at various temperatures. The Arrhenius plot of $R_{\max}/C_M$ is shown in Fig. 6. From the slope, an activation energy in the dimerization reaction was calculated to be 11.1 kcal/mol. Pillai *et al.* (*8*) obtained the activation energy of ethylene dimerization, 8.73 kcal/mol, when the

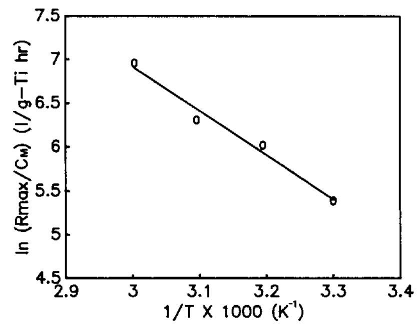

FIG. 6. Arrhenius plot of $R_{\max}/C_M$. Dimerization condition: Al/Ti molar ratio = 9.2, Ti = 1.33 mmol/liter.

TABLE 2

Maximum Rates of Dimerization with Various Temperatures at Initial Period (Dimerization Condition: Al/Ti = 9.2, Ti = 1.33 mmol/liter)

T (K)	P_M[a] (atm)	C_M[b] (mol C_2/liter)	R_{max} (g C_2^{2-}/g Ti hr)	R_{max}/C_M (g Ti/liter)$^{-1}$ hr
303	0.9186	0.1067	780	261
313	0.7985	0.0838	1175	501
323	0.6356	0.0607	1187	698
333	0.4192	0.0366	1524	1489

[a] P_M, partial pressure of ethylene.

[b] C_M, concentration of ethylene in the liquid phase.

Al/Ti molar ratio was 7.6 in *n*-heptane solvent.

Deactivation Rate in Dimerization Reaction

(1) *Effect of the Al/Ti molar ratio on the deactivation rate.* As mentioned earlier, products derived from titanium alkoxide and aluminum alkyl are complex and the main products are highly dependent on the Al/Ti molar ratio. The order of the deactivation rate is one in which the Al/Ti molar ratio is below 5, as shown in Fig. 7. The order of decay is 2 when Al/Ti molar ratio is above 5, as shown in Fig. 8. The change of the order of decay with different Al/Ti molar ratios was mentioned earlier by Beach and Kissin (*10*). The decay in the rate of dimerization can be interpreted as a deactivation of the active sites. Hence two different mechanisms of deactivation can be proposed as

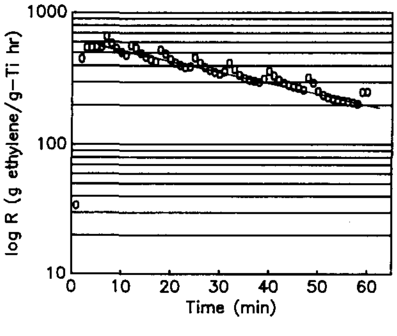

FIG. 7. Logarithmic plot of dimerization rate with reaction time. Dimerization condition: T = 303 K, P_t = 1.16 atm, Al/Ti molar ratio = 4.02.

$$C^* \xrightarrow[1^{st}\text{ order}]{\text{Al}} C_{d,1}, \quad \text{Al/Ti} < 5.0 \qquad (7)$$

$$2C^* \xrightarrow[2^{nd}\text{ order}]{\text{Al}} C_{d,2}, \quad \text{Al/Ti} > 5.0. \qquad (8)$$

$C_{d,1}$ in Eq. (7) can be proposed to have a structure (VI) where the linear Ti–C bond is lost by the further reaction of active site (complex (V)) with aluminum alkyl (*16*):

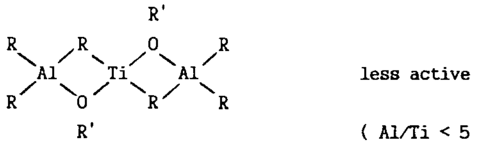

The complex (VI) could also dimerize ethylene to 1-butene in a different manner. The main step is a concerted coupling of two molecules of ethylene on a titanium atom affording titanium (IV) cyclopentane species, which then decompose to 1-butene by an intramolecular β-hydrogen transfer (*13*). The formation of 1-butene by the mechanism must occur slowly because a coplanar Ti–C–C–H arrangement is difficult to achieve (*20*).

When active sites deactivate in the second order with respect to the active site, dimerization rate profile during deactivation can be expressed as

$$1/R - 1/R_{max} = k_d'(t - t_{max}), \qquad (9)$$

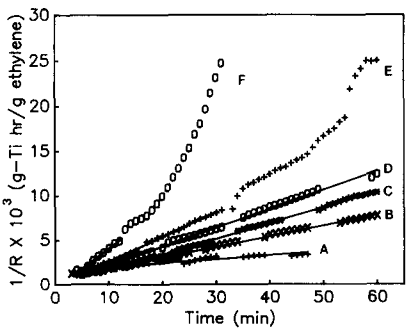

FIG. 8. Reciprocal plot of dimerization rates with reaction time at various Al/Ti molar ratios. Dimerization condition: T = 303 K, P_t = 1.16 atm, Ti = 1.33 mmol/liter, Al/Ti molar ratio of (A) 5.37; (B) 8.05; (C) 10.7 (D) 13.4; (E) 16.1; (F) 21.5.

where, $k_d' = (k_d/k_D)(1/C_M)$, (mol ethylene/liter)$^{-1}$, k_d is the second-order deactivation rate constant, (mol/liter)$^{-1}$ · hr^{-1}, and k_D is the dimerization rate constant, (mol/liter)$^{-1}$ · hr^{-1}.

The apparent deactivation rate constants, k_d', at various Al/Ti molar ratios, are shown in Table 3. As shown in Fig. 9, apparent decay rate constants are proportional to the concentration of triethyl aluminum. $C_{d,2}$ in Eq. (8) can be assumed to be a dimerized species of active sites from the reaction with aluminum alkyl as suggested in

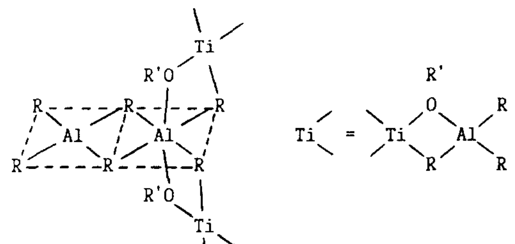

(VII) inactive species (Al/Ti > 5.0)

The structure of (VII) is analogous to the tetrameric aluminum alkoxide (*21*). Deactivation by agglomerization of active sites was suggested by Pillai *et al.* (*8*) when the Al/Ti molar ratio is greater than 10.6. At very high concentrations of aluminum alkyl, the tetramerization of active sites can form a structure like hexameric aluminum alkoxide (*21*). As shown in Fig. 8E and 8F, the order of deactivation is higher than 2, indicating the formation of inactive trimer and tetramer of active sites.

TABLE 3

Apparent Deactivation Rate Constants (k_d') at Various Al/Ti Molar Ratios (Dimerization Condition: T = 303 K, C_M = 0.1067 mol/liter)

Al/Ti (mol ratio)	k_d' (liter/mol C_2)	$k_d{}^*C_m$ (–)
5.4	1.156	0.1257
8.1	3.165	0.3377
9.2	3.798	0.4052
10.7	3.644	0.4729
13.4	5.583	0.5956
16.1	7.304	0.7794

(2) *Effect of monomer concentration.* Apparent decay rate constants at various monomer concentrations are shown in Table 4. The dimerization temperature is 323 K and the Al/Ti molar ratio was 9.2. The values of $k_d'{}^*C_M$ are nearly the same at different monomer concentrations, indicating that the deactivation is not influenced by monomer concentration.

(3) *Effect of temperature.* Table 5 shows apparent deactivation rate constants at various dimerization temperatures. The Arrhenius plot of $k_d'{}^*C_M$ is shown in Fig. 10. From

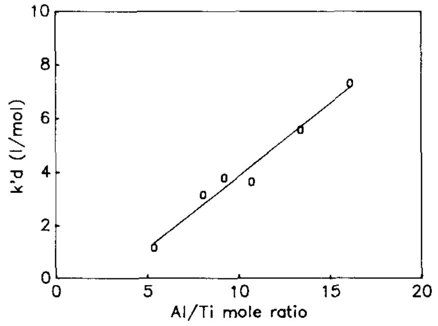

FIG. 9. Apparent deactivation rate constants (k_d') at various Al/Ti molar ratios. Dimerization condition: T = 303 K, C_M = 0.1067 *mol/liter.*

TABLE 4

Apparent Deactivation Rate Constants at Various Monomer Concentrations (Dimerization Condition: Al/Ti = 9.2, T = 323 K, [Ti] = 1.33 mmol/liter)

P_M (atm)	C_M (mol/liter)	k_d' (liter/mol C_2)	$k_d{*}C_M$ (−)
0.6356	0.0607	17.36	1.191
0.8685	0.0829	18.63	1.544
1.1014	0.1051	12.69	1.334

the slope of the Arrhenius plot of $k_d'{*}C_M$, activation energy of k_d' was calculated to be 9.4 kcal/mol. If the maximum rate of dimerization corresponds to the maximum number of active sites, Eq. (10) must be satisfied (see Eq. (9)):

$$E[k_d'] = E(k_d) - E(k_D), \qquad (10)$$

The activation energy of the deactivation rate can be calculated from the previously determined value of $E(k_D)$, 11.1 kcal/mol, to be 20.5 kcal/mol.

Determination of Active Sites Concentration

Various methods for determining the number of active centers in Ziegler–Natta catalysts have been recently reviewed by Tait (*22*). In our experiments the number of dimerization active centers was determined by the CO-poisoning method. When the CO-poisoning method was carried out at a Al/Ti molar ratio larger than 6, decay of dimerization rate was not clearly observed, because the decrease in the reaction rate due to CO poisoning of active sites cannot be separated from the deactivation due to aluminum alkyls. Hence the CO-poisoning method was carried out at a Al/Ti molar ratio of 5.4, where deactivation by excess aluminum alkyl was small. As shown in Fig. 11, the dimerization rate was not recovered after injection of CO, which is quite different from Ziegler–Natta olefin polymerization catalysts showing 70–85% recovery of activity after CO poisoning (*23*). Irreversible mechanism of CO poisoning can be proposed as

$$C^* + CO \rightarrow C_{d,CO}. \qquad (11)$$

On the assumption that one molecule of CO is adsorbed on each active site, the number of active sites can be calculated by extrapolation of the plots of percentage decrease in rate versus the amount of CO adsorbed to 100% decrease in rate. On the addition of a prescribed amount of CO into the reactor, the dimerization rate decreased

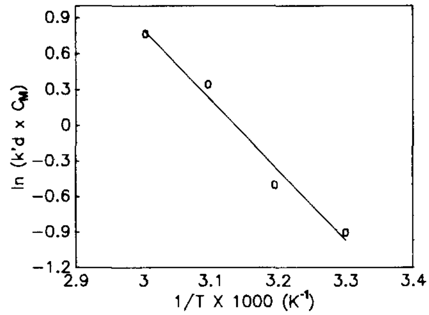

FIG. 10. Arrhenius plot of $k_d'{*}C_M$. Dimerization condition: Al/Ti molar ratio = 9.2, Ti = 1.33 mmol/liter.

TABLE 5

Apparent Deactivation Rate Constants at Various Temperatures (Dimerization Conditions: Al/Ti = 9.2, Ti = 1.33 mmol/liter)

T (K)	P_M (atm)	C_M (mol C_2/liter)	k_d' (liter/mol C_2^{2-})	$k_d'{*}C_M$ (−)
303	0.918	0.1067	3.79	0.405
313	0.798	0.0838	7.23	0.606
323	0.636	0.0607	19.62	1.191
333	0.419	0.0366	58.83	2.151

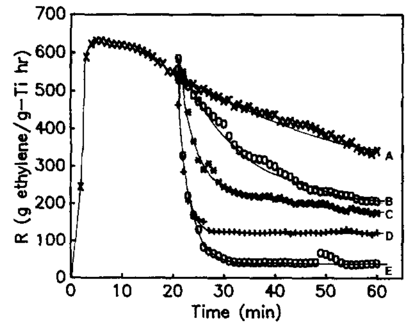

FIG. 11. Rate profiles induced by injections of CO during dimerization. Dimerization condition: $T = 303$ K $C_M = 0.1067$ mol/liter, Al/Ti molar ratio = 5.4. CO/Ti in mol%: (A) 0; (B) 3.84; (C) 6.14; (D) 8.64; (E) 10.67.

gradually and reached constant value after 20 min of CO injection ($R(i + 20)$). From the extrapolation as shown in Fig. 12, the number of active sites corresponding to the rate of dimerization at 20 min after injection of CO (420 g ethylene/g Ti hr) was calculated to about 12% of total Ti atom. The maximum rate of dimerization observed in our experiment is 1180 g ethylene/g Ti hr as shown Table 1. The maximum number of active sites ($[C^*]_{\max}$) can be estimated to be about 35% of the total titanium content. The number of active sites varies from 16% to 32% of total Ti atom depending on the Al/Ti molar ratio. The dimerization rate constant (k_D) can be estimated from the relation of $R_{D,\max} = k_D\, [C^*]_{\max}\, C_M$ to be 75.2 l/mol sec. This value is comparable with those of the unsupported catalysts for ethylene polymerization (*24*): 120 l/mol sec for $TiCl_3OCH_3$–$AlEt_3$ and 230 liter/mol sec for $TiCl_4$–$AlEt_3$ catalysts at 70°C.

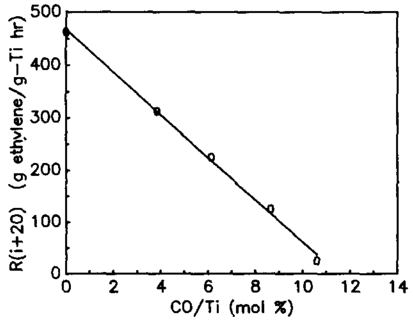

FIG. 12. Decrease in dimerization rates with the amount of CO injected. Dimerization condition is the same as that in Fig. 11.

CONCLUSION

The kinetic study of dimerization of ethylene catalyzed over $Ti(O\text{–}nC_4H_9)_4/AlEt_3$ was investigated in a semibatch reactor. The products contain exclusively 1-butene (>97%), hexenes (<2%), and solid product (<2%), which could indicate the uniformity of active sites for dimerization of ethylene to 1-butene. The effect of Al/Ti molar ratio on the initial dimerization rate profile allowed us to propose a mechanism for the formation of active sites; the primary active species, complex (V), is formed from the reaction of preactive sites, complex (IV), with aluminum alkyl. The order of deactivation is changed from 1 to 2 when the Al/Ti molar ratio is larger than 5. The mechanism of second-order deactivation can be explained by dimerization of active sites with aluminum alkyl; formation of complex (VII). The measurement of active sites by the CO-poisoning method showed that the maximum number of active sites was 35% of the total Ti content at 303 K and Al/Ti molar ratio of 5.4. The dimerization rate constant was calculated as 75.2 liter/mol sec at 303 K.

ACKNOWLEDGMENTS

The financial support of Yukong Co., Ltd. is greatly appreciated. The donation of titanium butoxide from Korea Petrochemical Ind. Co., Ltd. is also appreciated.

REFERENCES

1. Bawn, E. H., and Symcox, R., *J. Polym. Sci.* **34**, 139 (1959).
2. Takeda, M., Kimura, K., and Nozawa, Y., Koide, N., and Hisatome, M., *J. Polym. Sci. Part C* **23**, 741 (1968).
3. Wilke, G., *Angew. Chem.* **68**, 306 (1956).
4. Natta, N., *J. Polym. Sci.* **48**, 419 (1960).
5. Natta, G., Porri, L., Cabonaro, A., and Stoppa, G., *Makromol. Chem.* **77**, 112 (1964).
6. Natta, G., Porri, L., and Carbonaro, A., *Makromol. Chem.* **77**, 126 (1964).

7. Natta, G., Porri, L., and Valenti, S., *Makromol. Chem.* **67,** 225 (1963).

8. Pillai, S. M., Ravindranathan, M., and Sivaram, S., *Chem. Rev.* **86,** 353 (1986).

9. Beach, D. L., and Kissin, Y. V., *J. Polym. Sci. Polym. Chem. Ed.* **22,** 3027 (1984).

10. Beach, D. L., and Kissin, Y. V., *J. Polym. Sci. Polym. Chem. Ed.* **4,** 1069 (1986).

11. Bohm, L. L., *J. Appl. Polym. Sci.* **29,** 279 (1984).

12. Young, A. D., *J. Mol. Catal.* **53,** 433 (1989).

13. Commereuc, D., Chauvin, Y., Gaillard, J., Leonard, L., and Andrews, J., *Hydrocarbon Process,* 118 (1984).

14. Djabiev, T. S., Sabirova, R. D., and Shilov, A. E., *Kinet. Katal.* **5,** 441 (1964).

15. Hirai, H., Hiraki, K., Noguchi, I., and Makishima, S., *J. Polym. Sci. Part A-1* **8,** 147 (1970).

16. Christenson, C. P., May, J. A., and Freyer, L. E., *in* "Transition Metal Catalized Polymerization: Alkenes and Dienes" (R. P. Quirk, Ed.), p. 763. Harwood, New York, 1983.

17. Ledwith, A., and Sherrington, D. D., *in* "Reactivity, Mechanism and Structure in Polymer Chemistry" (A. D. Jenkins and A. Ledwith, Eds.), Chap. 12. Wiley, New York, 1974.

18. Kissin, Y. V., "Isospecific Polymerization of Olefins with Heterogeneous Ziegler-Natta Catalysts," Chap. 5. Springer-Verlag, New York, 1985.

19. Levenspiel, O., "Chemical Reaction Engineering," p. 185. Wiley, New York, 1972.

20. Crabtree, R. H., "The Organometallic Chemistry of the Transition Metals," p. 40. Wiley, New York, 1988.

21. Bradley, D. C., *in* "Inorganic Polymers" (F. G. A. Stone and W. A. G. Graham, Eds.), Chap. 7. Academic Press, New York, 1962.

22. Tait, P. J. T., *in* "Transition Metal Catalized Polymerization: Alkenes and Dienes" (R. P. Quirk, Ed.), p. 115. Harwood, New York, 1983.

23. Caunt, A. D., Davies, S., and Tait, P. J. T., *in* "Transition Metal Catalyzed Polymerization, Ziegler-Natta and Metathesis Polymerizations" (R. P. Quirk, Ed.), p. 105. Cambridge Univ. Press, New York, 1988.

24. Barbe, P. C., Cecchin, G., and Noristi, L., *Adv. Polym. Sci.* **81,** 1 (1987); and reference therein.